Synthesis A. El Khoury et al. Special Topic

Catalytic Synthesis of PEGylated EGCG Conjugates that Disaggregate Alzheimer's Tau

Anton El Khoury
Paul M. Seidler[1]
David S. Eisenberg*
Patrick G. Harran*

Department of Chemistry and Biochemistry, Molecular Biology Institute, Howard Hughes Medical Institute, University of California–Los Angeles, 607 Charles E. Young Drive East, Los Angeles, CA 90095-1569, USA
harran@chem.ucla.edu

Published as part of the
Special Issue dedicated to Prof. Sarah Reisman, recipient of the 2019 Dr. Margaret Faul Women in Chemistry Award

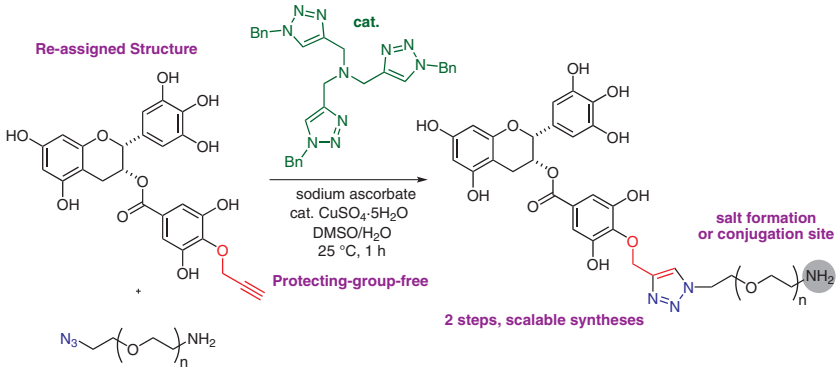

Received: 16.04.2021
Accepted after revision: 17.05.2021
Published online: 17.05.2021
DOI: 10.1055/a-1509-5904; Art ID: ss-2021-m0212-st

Abstract The naturally occurring flavonoid (–)-epigallocatechin gallate (EGCG) is a potent disaggregant of tau fibrils. Guided by the recent cryo-electron microscopy (cryoEM) structure of EGCG bound to fibrils of tau derived from an Alzheimer's brain donor, methods to site-specifically modify the EGCG D-ring with aminoPEGylated linkers are reported. The resultant molecules inhibit tau fibril seeding by Alzheimer's brain extracts. Formulations of aminoPEGylated EGCG conjugated to the (quasi)-brain-penetrant nanoparticle Ferumoxytol inhibit seeding by AD-tau with linker length affecting activity. The protecting group-free catalytic cycloaddition of amino azides to mono-propargylated EGCG described here provides a blueprint for access to stable nanoparticulate forms of EGCG potentially useful as therapeutics to eliminate Alzheimer's-related tau tangles.

Key words (–)-epigallocatechin gallate, Alzheimer's disease, tau disaggregation, nanoparticle conjugation, click reaction, TBTA

Alzheimer's disease (AD) is the 6th leading cause of death in the United States and 7th in the world. Personal and economic burdens associated with this most common type of dementia are enormous. Approximately 6.8 million Americans currently suffer from the disease. By 2050, its annual costs to the healthcare system are anticipated to reach $1.1 trillion.[2] Despite decades of research and numerous attempts at treatment, much is still unknown about the etiology of Alzheimer's. Two main markers have been identified: plaques of aggregated β-amyloid and neurofibrillary tangles of tau. However, the precise cause of cognitive decline and effective drug targets have been elusive. Early focus on β-amyloid led to clinical trials of multiple therapeutic candidates with limited success.[3] Those failed trials called into question the hypothesis that amyloid plaques play a decisive role in cognitive decline. Recent advances in imaging[4] showed tau tangles to be the best predictors of Alzheimer's progression as well as the species responsible for driving brain atrophy. Oligomeric and fibrillar tau appear to be promising targets for therapeutics.

The polyphenolic flavanoid (–)-epigallocatechin gallate (EGCG) inhibits aggregation of proteins involved in neurogenerative amyloidoses including huntingtin, amyloid-β, and α-synuclein.[5] Wobst et al.[6] reported EGCG blocks the fibrillization of tau by sequestering unfolded protein monomers. Recently, cryoEM was used to determine the binding site for EGCG on fibrils of tau deriving from the brain tissue of a donor with AD.[7] Relative to the apo AD-tau fibril, the bound form contains EGCG wedged into an interfacial cleft (Figure 1).

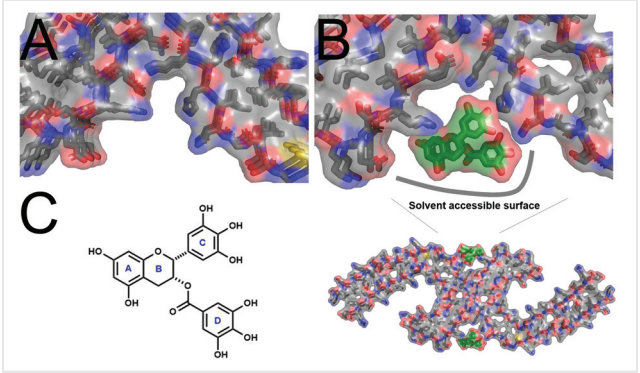

Figure 1 CryoEM structure of non-liganded AD-tau fibrils (**A**, PDB 6HRE) and fibrils bound to disaggregant EGCG (**B**), from reference 7a. EGCG is rendered green with oxygens shown in red. Residues from the Tau protein are rendered grey with oxygens red, nitrogens blue, and sulfur gold. The surface on EGCG that remains solvent accessible in the fibril-bound pose is labeled. **C**: Chemical structure of EGCG showing the nomenclature of ring systems. Density map of EGCG-tau binding cleft (green: EGCG, blue/grey: tau fibril).

Georg Thieme Verlag KG, Rüdigerstraße 14, 70469 Stuttgart, Germany

The structure of EGCG bound to AD tau indicated positions on the small molecule that might serve as anchor points for nanoparticle conjugation, wherein the ability to bind tau fibrils would be retained. Despite numerous reports of therapeutic potential for EGCG, the compound is prone to auto-oxidation, has poor pharmacokinetics, and is largely excluded from the brain when administered systemically. Stable conjugation to brain penetrant nanoparticles was seen as potential means to offset those limitations.[8] We selected Ferumoxytol as a nanoparticle carrier. Ferumoxytol exhibits moderate brain penetration, with penetration increasing coincident with pathologies that alter the neurovascular unit.

As best modeled (Figure 1B), the tau bound form of EGCG oriented its A-ring C5 phenol and a major portion of the gallate D-ring towards solvent. We sought to selectively derivatize the natural product ($ 17/g, Oakwood Chemicals) at one position along this periphery (see Scheme 1) with end-functionalized ethylene glycol chains of varying length.

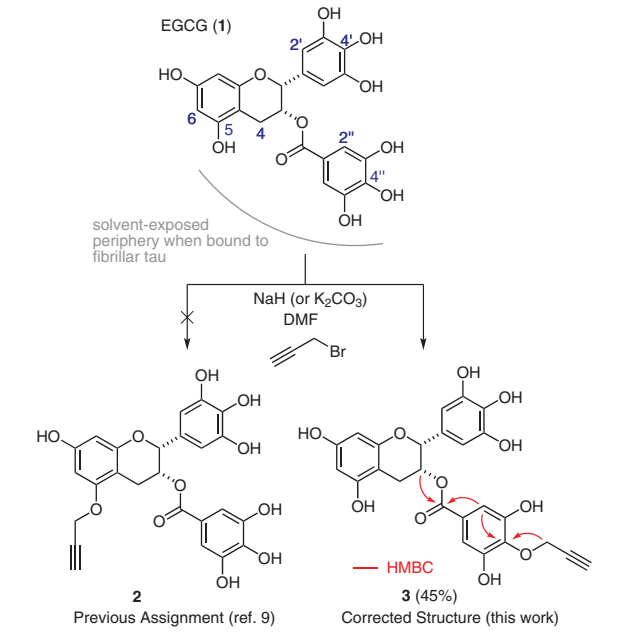

Scheme 1 Properly assigning the structure of mono-propargylated EGCG

Wang and co-workers had reported that a sodium salt of EGCG reacted with propargyl bromide in DMF at 80 °C to afford predominantly A-ring mono-ether **2**, along with lesser amounts of further propargylated compounds.[9] We repeated this reaction and found spectroscopic data for the major etherification product was inconsistent with structure **2**. HMBC spectra showed a correlation between the propargylic methylene protons (OCH_2, 4.76 ppm) and C-4″ (137.0 ppm). C4″ exhibited coupling with C2″-H (6.89 ppm), and C2″-H also correlated to the carbonyl carbon (165.7 ppm). C5 (95.2 ppm), the linkage site assigned in **2**, exhibited correlations to C6-H and the C4 methylene protons, but not to the propargyl group or D ring aryl protons. These data indicated the proper structure assignment should be the ether **3**, wherein alkylation had occurred at the *p*-OH of the gallate ester. This phenol is presumably the most acidic in EGCG.

A second product **3′** isolated from the reaction was doubly etherified (see SI for structure) and showed HMBC correlations between a second propargylic methylene (OCH_2, 4.67 ppm) and C4′ (137.0 ppm), and between C4′ and C2′-H (6.53 ppm). Data indicated the second propargyl ether formed on ring C. The phenols on ring A appeared to be the least susceptible to alkylation under basic conditions.

With the structure of **3** confirmed, conditions were screened to optimize its formation while avoiding the use of NaH in DMF – a potentially explosive combination, particularly when heated.[10] It was eventually found that treating EGCG with 1 equivalent of propargyl bromide and 0.5 equivalent of powdered K_2CO_3 in DMF at room temperature afforded **3** in 45% isolated yield – versus the 33% yield obtained using the NaH/DMF procedure.

We next synthesized a set of glycol based ω-amino azides **4a–e** with chain lengths varying from 5 to 17 atoms (see Table 2 and experimental section for details) in order to produce EGCG conjugates with incrementally increasing chain lengths. Cycloaddition reaction conditions were first optimized with **4c** using copper catalysis (Table 1).[11] Standard conditions[12] using catalytic Cu(II) and sodium ascorbate in aqueous THF (Table 1, entries 1, 2), failed to cycloadd **4c** to **3** due to substrate insolubility. When THF was replaced with *t*-BuOH, desired triazole **5c** was detected, but only in trace quantities (entry 3). An attempt to replace sodium ascorbate with Cu(0)[13] was unsuccessful (entry 4), as was the use of stoichiometric Cu(I) (entry 6). Notably, when stoichiometric amounts of $CuSO_4$ were employed (entry 5), starting materials were consumed and a highly insoluble precipitate formed. The use of H_2O/DMSO co-solvent mixture resulted in the formation of the product in 12% yield (entry 7), which remained unchanged even in the presence of excess amino azide partner (entry 8). We suspected this material was a copper/product complex and hypothesized that earlier attempts at catalysis may have been poisoned by **5c**. To fortify the copper catalyst against possible product sequestration, we turned to polydentate ligands reported by Sharpless.[14] Gratifyingly, in the presence tris[(1-benzyl-4-triazolyl)methyl]amine (TBTA), 20 mol% of $CuSO_4$ rapidly catalyzed the cycloaddition of **4c** to **3** in H_2O/DMSO at room temperature to afford triazole adduct **5c** in 52% isolated yield (entry 9). When the catalyst load was decreased from 20 to 5 mol%, isolated yield decreased, and conversion plateaued at roughly 80%. The reactions required no workup and product was easily purified as its TFA salt via preparative reverse-phase HPLC (see experimental section for details).

Table 1 Protecting Group-Free, Copper-Catalyzed Huisgen Cycloaddition to Form AminoPEGylated EGCG[a]

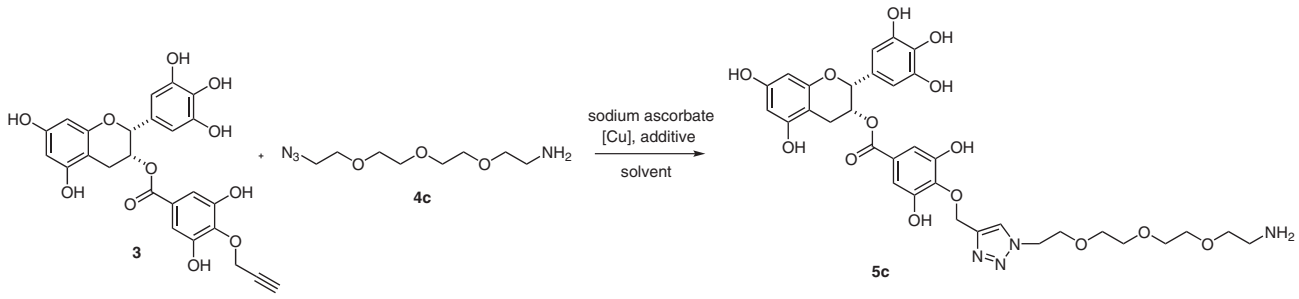

Entry	[Cu]	Additive	Solvent (4:1)	Yield (%)[b]
1	$Cu(OAc)_2$ (0.2 equiv)	–	H_2O/THF	0
2	$CuSO_4{\cdot}5H_2O$ (0.2 equiv)	–	H_2O/THF	0
3	$CuSO_4{\cdot}5H_2O$ (0.2 equiv)	–	H_2O/*t*-BuOH	trace
4[c]	$CuSO_4{\cdot}5H_2O$ (0.2 equiv)	–	H_2O/*t*-BuOH	0
5	$CuSO_4{\cdot}5H_2O$ (1 equiv)	–	H_2O/*t*-BuOH	–[d]
6[e]	CuBr (1 equiv)	–	H_2O/DMSO	–[f]
7	$CuSO_4{\cdot}5H_2O$ (0.5 equiv)	–	H_2O/DMSO	12
8[g]	$CuSO_4{\cdot}5H_2O$ (0.5 equiv)	–	H_2O/DMSO	12
9	**$CuSO_4{\cdot}5H_2O$ (0.2 equiv)**	**TBTA[h]**	**H_2O/DMSO**	**52**

[a] Reaction conditions: **3** (1 mmol), **4c** (1 mmol), [Cu], additive (50 mol%), sodium ascorbate (2.0 equiv), solvent (0.1 M), 1 h.
[b] Isolated yield.
[c] Cu (powder) was used as a reductant instead of sodium ascorbate.
[d] Reaction resulted in the formation of insoluble precipitate.
[e] No sodium ascorbate was added.
[f] Complex mixture.
[g] 2 mmol of **4c** were used.
[h] TBTA: Tris((1-benzyl-4-triazolyl)methyl)amine.

Table 2 A Set of EGCG Derivatives Having Varied Linker Lengths[a]

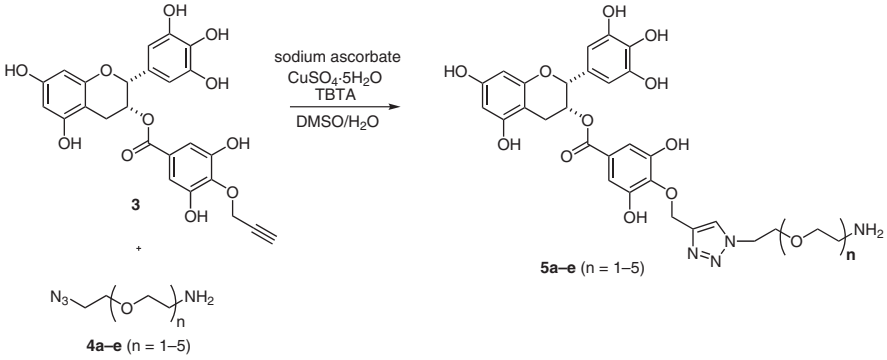

Compound	n	Yield (%)[b]
5a	1	68
5b	2	58
5c	3	52
5d	4	46
5e	5	45

Using the conditions shown in Table 1, entry 9, a set of EGCG conjugates having increasing chain lengths were synthesized (Table 2). As the number of glycol units increased, the yields of triazole products **5** decreased slightly. But in all cases, analytically pure product was isolated readily using preparative reversed phase HPLC.

Interestingly, when analyzing amine salts **5** by ^{1}H NMR in protic solvents (i.e., CD_3OD or D_2O), the aryl protons in the A-ring (5.93 ppm) quickly disappeared. Their integration (relative to stable resonances) decreased ~75% in 3 hours. Overnight storage of the NMR samples saw complete disappearance of both signals. HRMS identified the products as [M + 1] + 2 ions, indicating C–H bonds in the A ring had been replaced by C–D bonds. Notably, C–H bonds in the C and D rings showed no exchange, even after prolonged storage. Deuteration of flavonoids has been observed in the gas phase by mass spectrometry.[15] Jordheim and co-workers reported anthocyanidin natural products are deuterated in 15 vol% TFA in CD_3OD over a period of days.[16] Rapid deuteration of compounds **5** at room temperature may derive from the acidity of their amine salt appendages, wherein deuteration of the A-ring was presumably occurring via a dearomatized species of type **i** (Scheme 2). The A-ring appeared to be considerably more basic than the C and D rings. Along those lines, we observed that EGCG itself would react with *N*-iodosuccinimide to rapidly and selectively iodinate the A-ring (data not shown).

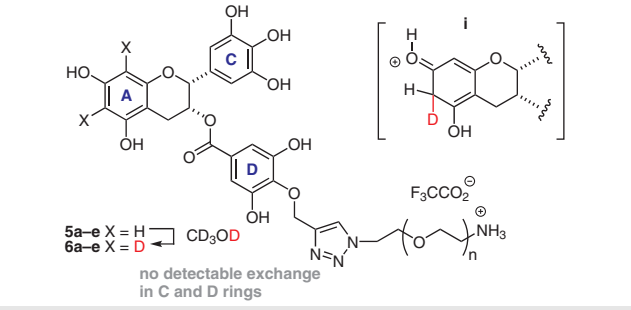

Scheme 2 Rapid and selective A-ring deuteration of EGCG conjugates

We next tested if the D-ring site of triazole-linked aminoPEGylation would interfere with tau fibril disaggregation observed for EGCG. AD crude brain extracts have been shown to seed aggregation of fluorescently labeled tau in HEK293 recipient biosensor cells expressing an aggregation-prone fragment of tau called K18,[17] and seeding is inhibited by EGCG.[7a] We compared inhibition of seeding by EGCG and D-ring analogues **5a–c** as a preliminary proof-of-concept. Crude extract of autopsied brain tissue of a donor with AD (prepared as described in the SI) were pre-incubated with inhibitors (10 μM final concentration on cells) for 16–18 hours and resulting homogenates were added to the cells for imaging 3 days later. The data obtained are shown in Figure 2.

Intracellular tau aggregates are seen as bright green puncta in cells that were seeded with crude AD brain extract in the absence of inhibitor. The number of puncta in inhibitor-treated cells are a proxy used to assess the disaggregating activity of EGCG-linked nanoparticles. To our delight, all of the EGCG-linker conjugates inhibited seeding by AD brain extracts by at least 90% with **5c** displaying potency nearly on par with EGCG itself. As a comparison with other analogues of EGCG, we tested ECG, which lacks the *meta*-OH group of the C ring. Consistent with the structure of EGCG bound to tau, which shows no contact with the *meta*-OH, ECG was seen to inhibit seeding as well as the linker-conjugated analogues and nearly as well as the parent natural product, EGCG. These data demonstrate that D ring derivatizations are well tolerated, consistent with our observation that the D ring remains largely solvent-exposed in the binding cleft of tangled tau filaments from AD brain.

EGCG is subject to off-target binding and rapid metabolism, which restricts its therapeutic potential. We reason that covalent conjugation of EGCG to nanoparticles may re-

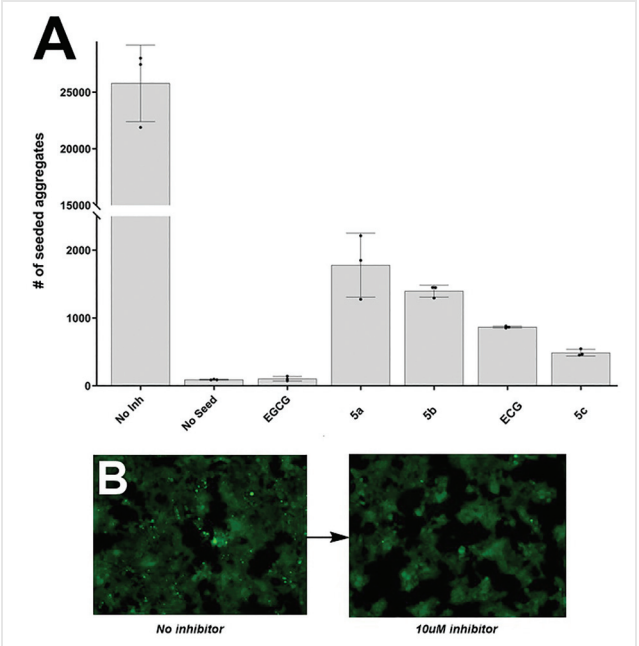

Figure 2 Linker conjugated EGCG analogues retain inhibitory activity towards AD crude brain extracts. **A**: Seeding by crude AD brain extract pre-treated with EGCG or experimental linker-conjugated analogues, as indicated. Inhibitor activity is read-out by measuring seeding in tau biosensor cells. Seeding is taken as a proxy for the fibril load that is contained within the AD crude brain extracts. Reduction in fibril load following treatment with experimental linker-conjugated analogues of EGCG reduces prion-like seeding by AD-tau nearly as effectively as EGCG itself. **B**: Representative fluorescence images of tau biosensor cells experiments from **A**. Intracellular aggregates seeded by crude AD brain extracts are identified as puncta (green dots in the 'No inhibitor' treated sample, left fluorescence micrograph). Inhibitor treatment reduces the number of puncta (right fluorescence micrograph). The number of puncta as a function of inhibitor pre-treatment is plotted in **A**.

duce binding to metabolic and off-target proteins, which accommodate EGCG inside of buried active sites of globular proteins that are sterically inaccessible to nanoparticle-bound molecules of EGCG. Thus, we sought to synthesize a series of EGCG-nanoparticle conjugates that varied by linker length to identify a minimal linker that retains interaction of EGCG with the solvent exposed binding cleft of fibrillar tau.

Ferumoxytol is an FDA approved carbohydrate-coated iron nanoparticle with widespread use in the clinic with applications ranging from anemia treatment to off-label MR imaging of neurovasculature.[8a,b,d,18] We conjugated an expanded series of EGCG bearing linkers of incrementally increasing length, **5a**–**e**, to Ferumoxytol nanoparticles using standard amidation conditions (sulfo-NHS, EDC, 2 h, rt). Unlike previous inclusion-based, labile EGCG nanoparticle formulations that release EGCG at sites of action,[19] we loaded the small molecule via covalent attachment. Covalent conjugation is likely to reduce off-target binding and has added potential to improve potency by exploiting the multivalency of the nanoparticle (each nanoparticle displays ~50 potential linking sites).

We tested the activity of Ferumoxytol conjugated EGCG analogues using the biosensor cell assay described above, except we omitted the pre-incubation step such that our assay more closely resembled the scenario of therapeutic intervention, for which there is no pre-incubation period. Nanoparticle conjugated EGCG derivative was mixed with crude AD brain extract and immediately transfected into tau biosensor cells. We find that all the analogues except for the compound with the shortest linker **5a** exhibited desired activity inhibiting seeding by at least 50% (Figure 3A). Overall, our data demonstrate that nanoparticle conjugates retain the inhibitory properties of the parent compound, and underscores that functional EGCG nanoparticles can be successfully designed based on information that is gleaned from the cryoEM structure.

As added evidence of its inhibitory action, we also observed an interesting effect of EGCG nanoparticle incubation with tau paired helical filaments purified from AD brain by negative-stain electron microscopy. Nanoparticles loaded with **5c** form dense clouds that engulf AD-tau fibrils, in some cases apparently unwinding the paired helical filament (Figure 3B). Non-conjugated control nanoparticles exhibited no apparent interaction with AD-tau fibrils (Figure 3C).

In summary, we have optimized a monoetherification of naturally occurring EGCG and properly assigned the regiochemistry of the reaction. We have established a procedure to directly catalyze cycloaddition of glycol based ω-amino azide chains to this molecule. The resultant amino polyphenolic conjugates retain the ability to disaggregate AD brain-derived tau – both as isolated species and when loaded onto Ferumoxytol nanoparticles. These promising results provide a blueprint for future work wherein further refinements to the EGCG molecule and optimized nanoparticulate formulations could provide means to deliver a potent tau fibril disaggregant to the brains of Alzheimer's patients.

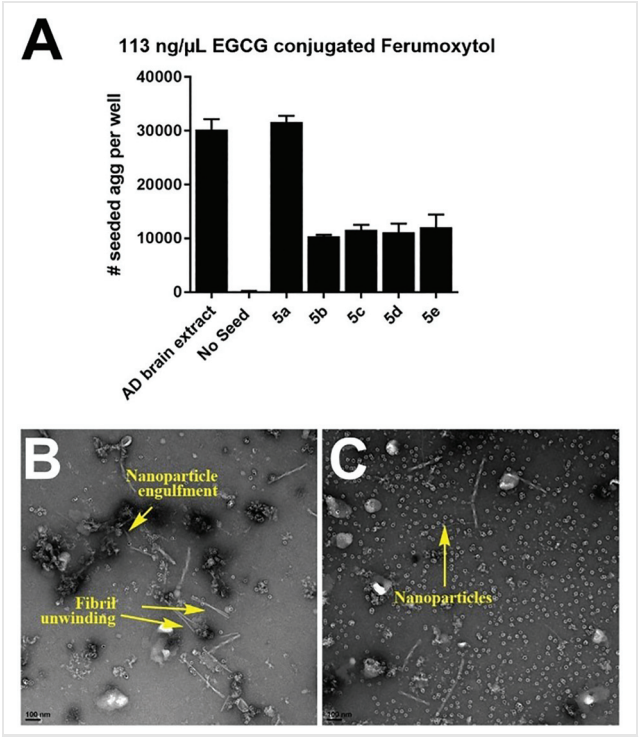

Figure 3 Nanoparticle-conjugated EGCG retains inhibitor activity and clusters with fibrils of AD-tau. **A**: Seeding by crude AD brain extract measured in tau biosensor cells that were co-transfected with nanoparticles coupled to EGCG by linkers of varying length. **B**, **C**: Negative-stain electron micrographs of EGCG-conjugated and non-conjugated nanoparticles. Nanoparticle coupled with EGCG analogue **5c** (**B**) cluster with fibrils of AD-tau. No clustering is seen between non-conjugated nanoparticles and AD-tau fibrils (**C**).

All reagents were purchased from commercial suppliers (Sigma-Aldrich, Combi-Blocks, or Oakwood Chemicals) and were used without further purification. When necessary, reaction solvents were dried using an activated alumina solvent drying system. TLC was performed on pre-coated plates Sorbent Technologies, silica gel 60 PF_{254} (0.25 mm). TLC plates were visualized with UV light (254 nm) or stained using $KMnO_4$ or ninhydrin. Flash chromatography was performed on silica gel 60 (240–400 mesh). Purification of final products was performed using an Agilent 1200 HPLC system equipped with G1361A preparative pumps, and a Waters Sunfire C18 column (5 µm, 19 mm × 250 mm). Analytical HPLC was performed using the same system, but with a G1312A binary pump. NMR spectra were recorded on a Bruker Avance (500 MHz) spectrometer using $CDCl_3$ or CD_3OD as solvents and referenced relative to residual $CHCl_3$ (δ = 7.26) or CD_3OD (δ = 3.31). Chemical shifts are reported in ppm and coupling constants *J* in hertz (Hz). ^{13}C NMR spectra were recorded on the same instruments (125 MHz) with total proton decoupling referenced relative to residual $CHCl_3$ (δ = 77.16) or CD_3OD (δ = 49.00). IR spectra were

obtained on Jasco FT/IR-4100 equipped with a universal ATR sampling accessory. High-resolution mass spectra were recorded on Waters LCT Premier. Optical rotations were measured on a Rudolph Autopol III Automatic Polarimeter and are quoted in units of degree.

Experimental procedures for biological studies are provided in the Supporting Information.

Amino Azides 4; General Procedure 1 (GP1)

The corresponding diol (1.0 equiv) was dissolved in DCM (0.6 M), followed by the addition of TsCl (2.1 equiv). The reaction was cooled to 0 °C. KOH (8.0 equiv) was then added in one portion, the reaction mixture was warmed to rt and stirred for 4 h. The mixture was then diluted with H_2O (100 mL) and extracted with DCM (3 × 100 mL). The combined organic layers were dried ($MgSO_4$), filtered, and concentrated in vacuo. The crude bis-tosylate was obtained as a white solid and used directly in the next step.

To the crude bis-tosylate (1.0 equiv) in DMF (0.6 M) under argon was added NaN_3 (4.0 equiv). The reaction was stirred overnight at 80 °C. The mixture was then cooled to rt, diluted with H_2O (100 mL), and extracted with EtOAc (3 × 100 mL). Combined organic layers were washed with H_2O (2 × 50 mL) and brine (2 × 50 mL), dried ($MgSO_4$), filtered, and concentrated in vacuo. The resulting bis-azide was used directly in the next step without purification.

Crude bis-azide from the previous step (1.0 equiv) was dissolved in THF/Et_2O/H_2O (5:1:5, 0.6 M). PPh_3 (1.0 equiv) in Et_2O (0.7 M) was then added over 1 h using a syringe pump. The resulting solution was stirred at rt overnight at which time precipitate formation was observed. The reaction mixture was diluted with H_2O (100 mL) and washed with Et_2O (3 × 100 mL). The aqueous layer was then basified via the addition of solid NaOH to pH 11 and extracted with DCM (3 × 100 mL). Combined organic layers were dried ($MgSO_4$), filtered, and concentrated in vacuo. The crude product (TLC: DCM/MeOH 8:2 R_f = 0.2) was purified via flash column chromatography (silica gel, DCM/MeOH/Et_3N 100:0:0 to 90:10:0 to 80:10:10) to give the desired amino azide.

2-(2-Azidoethoxy)ethan-1-amine (4a)[20]

Compound was prepared according to GP1; starting with 849 mg (8.0 mmol) of diethylene glycol: yield: 936 mg (90%); yellow oil.

^{1}H NMR (500 MHz, $CDCl_3$): δ = 3.65 (t, *J* = 5.0 Hz, 2 H, 4-H), 3.54 (t, *J* = 5.1 Hz, 2 H, 2-H), 3.38 (t, *J* = 5.0 Hz, 2 H, 5-H), 2.90 (t, *J* = 5.1 Hz, 2 H, 1-H), 2.40 (s, 2 H, NH_2).

^{13}C NMR (125 MHz, $CDCl_3$): δ = 72.7, 70.0, 50.7, 41.6.

2-[2-(2-Azidoethoxy)ethoxy]ethan-1-amine (4b)[21]

Compound was prepared according to GP1; starting with 2.3 g (15.0 mmol) of triethylene glycol; yield: 2.35 g (90%); yellow oil.

^{1}H NMR (500 MHz, $CDCl_3$): δ = 3.68–3.63 (m, 6 H, 4-H, 5-H, 8-H), 3.53 (t, *J* = 5.0 Hz, 2 H, 2-H), 3.39 (t, *J* = 5.2 Hz, 2 H, 6-H), 2.88 (t, *J* = 5.0 Hz, 2 H, 1-H), 2.17 (s, 2 H, NH_2).

^{13}C NMR (125 MHz, $CDCl_3$): δ = 73.0, 70.7, 70.3, 70.1, 50.7, 41.6.

2-{2-[2-(2-Azidoethoxy)ethoxy]ethoxy}ethan-1-amine (4c)[22]

Compound was prepared according to GP1; starting with 2.62 g (13.5 mmol) of tetraethylene glycol; yield: 2.5 g (85%); yellow oil.

^{1}H NMR (500 MHz, $CDCl_3$): δ = 3.68–3.60 (m, 10 H, 3-H, 4-H, 5-H, 6-H, 7-H), 3.50 (t, *J* = 5.1 Hz, 2 H, 2-H), 3.39 (t, *J* = 5.1 Hz, 2 H, 8-H), 2.86 (t, *J* = 5.1 Hz, 2 H, 1-H), 1.89 (s, 2 H, NH_2)

^{13}C NMR (125 MHz, $CDCl_3$): δ = 73.1, 70.71, 70.66, 70.6, 70.3, 70.1, 50.7, 41.7.

14-Azido-3,6,9,12-tetraoxatetradecan-1-amine (4d)[23]

Compound was prepared according to GP1; starting with 3.39 g (14.2 mmol) of pentaethylene glycol; yield: 2.7 g (73%); yellow oil.

^{1}H NMR (500 MHz, $CDCl_3$): δ = 3.72–3.60 (m, 14 H, 3-H, 4-H, 5-H, 6-H, 7-H, 8-H, 9-H), 3.55 (t, *J* = 3.0 Hz, 2 H, 2-H), 3.38 (t, *J* = 4.7 Hz, 2 H, 10-H), 2.90 (t, *J* = 4.7 Hz, 2 H, 1-H).

^{13}C NMR (125 MHz, $CDCl_3$): δ = 71.9, 70.7–70.0 (wide peak), 50.7, 41.4.

17-Azido-3,6,9,12,15-pentaoxaheptadecan-1-amine (4e)[24]

Compound was prepared according to GP1; starting with 3.0 g (10.6 mmol) of hexaethylene glycol; yield: 2.27 g (70%); yellow oil.

^{1}H NMR (500 MHz, $CDCl_3$): δ = 3.96 (t, *J* = 3.2 Hz, 2 H, 11-H), 3.62–3.80 (m, 18 H, 2-H, 3-H, 4-H, 5-H, 6-H, 7-H, 8-H, 9-H, 10-H), 3.50 (t, *J* = 4.90 Hz, 2 H, 12-H), 3.15 (t, *J* = 4.90 Hz, 2 H, 1-H).

^{13}C NMR (125 MHz, $CDCl_3$): δ = 70.6–69.8 (wide peak), 66.9, 50.7, 40.6.

(2*R*,3*R*)-5,7-Dihydroxy-2-(3,4,5-trihydroxyphenyl)chroman-3-yl 3,5-Dihydroxy-4-(prop-2-yn-1-yloxy)benzoate (3) and (2*R*,3*R*)-2-[3,5-Dihydroxy-4-(prop-2-yn-1-yloxy)phenyl]-5,7-dihydroxychroman-3-yl 3,5-Dihydroxy-4-(prop-2-yn-1-yloxy)benzoate (3′)

Using NaH/DMF: To NaH (15.7 mg, 0.65 mmol, 1.5 equiv) at 0 °C was added a solution of EGCG (200 mg, 0.44 mmol, 1.0 equiv) in anhyd DMF (1.45 mL, 0.3 M). The resulting mixture was stirred at rt for 30 min. Propargyl bromide (53 µL, 0.48 mmol, 1.1 equiv, 80% w/w) was then added and the reaction mixture was heated to 80 °C and stirred overnight. Upon cooling to rt, the mixture was concentrated in vacuo and subjected to flash column chromatography (silica gel, $CHCl_3$/MeOH 100:0 to 15:1 to 13:1 to 11:1). Desired mono-propargylated product (TLC: $CHCl_3$/MeOH 8:2, R_f = 0.3) was obtained in 33% yield (72 mg) along with 15% (35 mg) of bispropargylated product (R_f = 0.6) as white solids.

Monopropargylated Product 3

Mp, decomposed at >120 °C; $[\alpha]_D^{21}$ –162.0 (*c* = 0.1, MeOH).

FT-IR (neat): 3358, 3290, 2124, 1697, 1606, 1522, 1454, 1371, 1347, 1242, 1196, 1147, 1056, 1039, 1017, 826, 769, 640 cm^{-1}.

^{1}H NMR (500 MHz, CD_3OD): δ = 6.89 (s, 2 H, Gal H-2, H-6), 6.47 (s, 2 H, H-2′, H-6′), 5.93 (s, 2 H, H-6, H-8), 5.52 (m, 1 H, H-3), 4.95 (s, 1 H, H-2), 4.76 (d, *J* = 2.4 Hz, 2 H, OCH_2R), 2.99–2.94 (dd, *J* = 17.3, 4.5 Hz, 1 H, H-4α), 2.85–2.80 (dd, *J* = 17.3, 2.3 Hz, 1 H, H-4β), 2.77 (t, *J* = 2.4 Hz, 1 H, ≡CH).

^{13}C NMR (125 MHz, CD_3OD): δ = 165.7, 156.5, 156.4, 155.8, 150.5, 145.3, 137.0, 132.4, 129.3, 125.7, 108.7, 105.4, 97.9, 95.2, 94.5, 78.6, 77.1, 75.3, 68.9, 58.6, 25.4.

HRMS (ESI): *m*/*z* calcd for $C_{25}H_{20}O_{11}$ [M + H]$^+$: 497.1039; found: 497.1102.

Bispropargylated Product 3′

Mp, decomposed at >120 °C; $[\alpha]_D^{21}$ –133.0 (*c* = 0.1, MeOH).

FT-IR (neat): 3359, 3282, 2926, 2858, 2362, 2124, 1695, 1601, 1519, 1451, 1363, 1235, 1174, 1142, 1049, 1014, 982, 754, 736, 711, 632 cm^{-1}.

^{1}H NMR (500 MHz, CD_3OD): δ = 6.88 (s, 2 H, Gal H-2, H-6), 6.50 (s, 2 H, H-2′, H-6′), 5.94 (s, 2 H, H-6, H-8), 5.55 (m, 1 H, H-3), 4.99 (s, 1 H, H-2), 4.76 (d, *J* = 2.4 Hz, 2 H, OCH_2R), 4.66 (d, *J* = 2.4 Hz, 2 H, OCH_2R′), 3.01–2.95 (dd, *J* = 17.4, 4.6 Hz, 1 H, H-4α), 2.86–2.81 (dd, *J* = 17.3, 2.2 Hz, 1 H, H-4β), 2.77 (t, *J* = 2.4 Hz, 1 H, ≡CH), 2.71 (t, *J* = 2.4 Hz, 1 H, ≡CH′).

^{13}C NMR (125 MHz, CD_3OD): δ = 165.6, 156.6, 156.5, 155.6, 150.5, 150.4, 137.0, 134.8, 132.3, 125.6, 108.7, 105.5, 97.9, 95.2, 94.5, 79.0, 78.6, 78.1, 75.3, 75.0, 68.8, 58.8, 58.6, 26.4.

HRMS (ESI): *m*/*z* calcd for $C_{28}H_{23}O_{11}$ [M + H]$^+$: 535.1240; found: 535.1252.

Using K_2CO_3/DMF: To EGCG (1 g, 2.18 mmol, 1.0 equiv) in DMF (11 mL, 0.2 M) at 0 °C was added K_2CO_3 (166 mg, 1.2 mmol, 0.5 equiv) in one portion. The reaction was stirred at rt for 1 h. Propargyl bromide (0.24 mL, 2.18 mmol, 1.1 equiv, 80% w/w) was then added and the mixture was stirred at the same temperature overnight. The mixture was then concentrated in vacuo and purified as above furnishing the product in 45% yield (491 mg) along with 10% of bispropargylated side product. All the analytical data matched the one obtained using the above alternative procedure.

Click Reaction with PEGylated Linkers; General Procedure 2 (GP2)

To a flame-dried microwave vial was added **3** (40 mg, 0.081 mmol, 1.0 equiv) and the corresponding azide **4** (0.081 mmol, 1.0 equiv). In a separate vial, a solution of $CuSO_4{\cdot}5H_2O$ (4 mg, 0.016 mmol, 0.2 equiv), sodium ascorbate (34 mg, 0.17 mmol, 2.0 equiv), and TBTA (21 mg, 0.04 mmol, 0.5 equiv) in DMSO/H_2O (4:1, 0.81 mL, 0.1 M) was prepared and added to the first vial. The reaction was stirred at rt for 1 h. The crude mixture was purified by preparative reverse-phase HPLC (33–60% MeCN/H_2O + 0.1% (v/v) TFA in 8.5 min] to give the desired triazole adduct **5** (t_R = 5.2 min).

(2*R*,3*R*)-5,7-Dihydroxy-2-(3,4,5-trihydroxyphenyl)chroman-3-yl 4-({1-[2-(2-Aminoethoxy)ethyl]-1*H*-1,2,3-triazol-4-yl}methoxy)-3,5-dihydroxybenzoate (5a)

Compound was prepared according to GP2; yield: 35 mg (68%); white solid; mp, decomposed at >120 °C; $[\alpha]_D^{21}$ –81 (*c* = 0.1, MeOH).

FT-IR (neat): 3374, 2951, 2934, 1676, 1626, 1523, 1448, 1370, 1196, 1146, 1061, 1015, 770, 724, 650, 612 cm^{-1}.

^{1}H NMR (500 MHz, CD_3OD): δ = 7.88 (s, 1 H, triazole-H), 6.87 (s, 2 H, Gal H-2, H-6), 6.50 (s, 2 H, H-2′, H-6′), 5.95 (s, 2 H, H-6, H-8), 5.54 (m, 1 H, H-3), 5.25 (s, 2 H, OCH_2R), 4.97 (s, 1 H, H-2), 4.56 (t, *J* = 4.8 Hz, 2 H, NCH_2CH$_2$OCH$_2$CH$_2$NH$_2$), 3.83–3.75 (m, 2 H, NCH$_2$CH_2OCH$_2$CH$_2$NH$_2$), 3.50–3.48 (m, 2 H, NCH$_2$CH$_2$OCH_2CH$_2$NH$_2$), 3.01–2.97 (m, 3 H, NCH$_2$CH$_2$OCH$_2$CH_2NH$_2$, and H-4α), 2.86–2.82 (dd, *J* = 17.3, 2.2 Hz, 1 H, H-4β).

^{13}C NMR (125 MHz, CD_3OD): δ = 165.6, 156.5, 156.5, 155.8, 150.4, 145.3, 137.1, 132.3, 129.4, 125.7, 124.9, 108.8, 105.4, 97.8, 95.1, 94.5, 77.0, 69.1, 69.0, 66.3, 63.9, 49.9, 39.0, 25.4.

HRMS (ESI): *m*/*z* calcd for $C_{29}H_{32}N_4O_{12}$ [M + H]$^+$: 627.1938; found: 627.1954.

(2*R*,3*R*)-5,7-Dihydroxy-2-(3,4,5-trihydroxyphenyl)chroman-3-yl 4-[(1-{2-[2-(2-Aminoethoxy)ethoxy]ethyl}-1*H*-1,2,3-triazol-4-yl)methoxy]-3,5-dihydroxybenzoate (5b)

Compound was prepared according to GP2; yield: 32 mg (58%); white solid; mp, decomposed at >120 °C; $[\alpha]_D^{21}$ –73 (*c* = 0.1, MeOH).

FT-IR (neat): 3170, 2964, 2952, 1678, 1627, 1609, 1523, 1450, 1376, 1347, 1201, 1146, 1058, 1039, 969, 836, 720, 677, 602 cm^{-1}.

^{1}H NMR (500 MHz, CD_3OD): δ = 7.90 (s, 1 H, triazole-H), 6.88 (s, 2 H, Gal H-2, H-6), 6.50 (s, 2 H, H-2′, H-6′), 5.95 (s, 2 H, H-6. H-8), 5.53–5.52 (m, 1 H, H-3), 5.26 (s, 2 H, OCH_2R), 4.97 (s, 1 H, H-2), 4.52–4.50 (t, *J* = 4.6 Hz, 2 H, NCH_2CH$_2$OCH$_2$CH$_2$OCH$_2$CH$_2$NH$_2$), 3.82–3.73 (m, 2 H, NCH$_2$CH_2OCH$_2$CH$_2$OCH$_2$CH$_2$NH$_2$), 3.50–3.48 (m, 2 H, NCH$_2$CH$_2$OCH$_2$CH$_2$OCH_2CH$_2$NH$_2$), 3.41 (m, 4 H, NCH$_2$CH$_2$OCH_2CH_2OCH$_2$CH$_2$NH$_2$), 3.02–2.96 (m, 3 H, NCH$_2$CH$_2$OCH$_2$CH$_2$OCH$_2$CH_2NH$_2$ and H-4α), 2.86–2.82 (dd, *J* = 18.1, 1.9 Hz, 1 H, H-4β).

^{13}C NMR (125 MHz, CD_3OD): δ = 165.6, 156.54, 156.46, 155.8, 150.4, 145.3, 137.1, 132.3, 129.4, 125.6, 108.9, 105.3, 97.8, 95.1, 94.5, 77.0, 70.1, 69.8, 68.98, 68.95, 66.3, 63.8, 53.7, 50.1, 39.3, 25.5.

HRMS (ESI): *m*/*z* calcd for $C_{31}H_{35}N_4O_{13}$ [M + H]$^+$: 671.2201; found: 671.2170.

(2*R*,3*R*)-5,7-Dihydroxy-2-(3,4,5-trihydroxyphenyl)chroman-3-yl 4-{[1-(2-{2-[2-(2-Aminoethoxy)ethoxy]ethoxy}ethyl)-1*H*-1,2,3-triazol-4-yl]methoxy}-3,5-dihydroxybenzoate (5c)

Compound was prepared according to GP2; yield: 30 mg (52%); white solid; mp, decomposed at >120 °C; $[\alpha]_D^{21}$ –62 (*c* = 0.1, MeOH).

FT-IR (neat): 3203, 2970, 1674, 1602, 1523, 1437, 1368, 1200, 1143, 1060, 981, 831, 718, 647, 622, 610 cm^{-1}.

^{1}H NMR (500 MHz, CD_3OD): δ = 7.87 (s, 1 H, triazole-H), 6.89 (s, 2 H, Gal H-2, H-6), 6.50 (s, 2 H, H-2′, H-6′), 5.94 (s, 2 H, H-6. H-8), 5.54–5.53 (m, 1 H, H-3), 5.25 (s, 2 H, OCH_2R), 4.97 (s, 1 H, H-2), 4.52 [t, *J* = 4.9 Hz, 2 H, NCH_2CH$_2$(OCH$_2$CH$_2$)$_2$OCH$_2$CH$_2$NH$_2$], 3.81–3.73 [m, 2 H, NCH$_2$CH_2(OCH$_2$CH$_2$)$_2$OCH$_2$CH$_2$NH$_2$], 3.59–3.57 [m, 2 H, NCH$_2$CH$_2$(OCH$_2$CH$_2$)$_2$OCH$_2$CH_2NH$_2$], 3.54–3.47 [m, 4 H, N-CH$_2$CH$_2$(OCH_2CH$_2$)$_2$OCH$_2$CH$_2$NH$_2$], 3.45–3.42 [m, 4 H, NCH$_2$CH$_2$(OCH$_2$CH_2)$_2$OCH$_2$CH$_2$NH$_2$], 3.07–3.05 [t, *J* = 5.5 Hz, 2 H, NCH$_2$CH$_2$(OCH$_2$CH$_2$)$_2$OCH$_2$CH_2NH$_2$], 3.01–2.96 (dd, *J* = 17.3, 4.5 Hz, 1 H, H-4α), 2.86–2.82 (dd, *J* = 17.3, 2.3 Hz, 1 H, H-4β).

^{13}C NMR (125 MHz, CD_3OD): δ = 165.6, 156.54, 156.48, 155.8, 150.4, 145.3, 137.0, 132.3, 129.4, 125.6, 124.9, 108.9, 105.3, 97.8, 95.1, 94.5, 77.0, 70.0, 69.9, 69.6, 69.0, 66.3, 63.9, 50.1, 39.3, 25.5.

HRMS (ESI): *m*/*z* calcd for $C_{33}H_{38}N_4O_{14}Na$ [M + Na]$^+$: 737.2282; found: 737.2308.

(2*R*,3*R*)-5,7-Dihydroxy-2-(3,4,5-trihydroxyphenyl)chroman-3-yl 4-{[1-(14-Amino-3,6,9,12-tetraoxatetradecyl)-1*H*-1,2,3-triazol-4-yl]methoxy}-3,5-dihydroxybenzoate (5d)

Compound was prepared according to GP2; yield: 28 mg (46%); white solid; mp, decomposed at >120 °C; $[\alpha]_D^{21}$ –69 (*c* = 0.1, MeOH).

FT-IR (neat): 3179, 2926, 1681, 1627, 1523, 1451, 1372, 1349, 1203, 1146, 1061, 1038, 831, 726, 641, 618 cm^{-1}.

^{1}H NMR (500 MHz, CD_3OD): δ = 7.90 (s, 1 H, triazole-H), 6.87 (s, 2 H, Gal H-2, H-6), 6.48 (s, 2 H, H-2′, H-6′), 5.93 (s, 2 H, H-6, H-8), 5.52–5.53 (m, 1 H, H-3), 5.23 (s, 2 H, OCH_2R), 4.95 (s, 1 H, H-2), 4.51–4.48 [t, *J* = 4.7 Hz, 2 H, NCH_2CH$_2$(OCH$_2$CH$_2$)$_3$OCH$_2$CH$_2$NH$_2$], 3.78–3.70 [m, 2 H, NCH$_2$CH_2(OCH$_2$CH$_2$)$_3$OCH$_2$CH$_2$NH$_2$], 3.61–3.58 [m, 2 H, NCH$_2$CH$_2$(OCH$_2$CH$_2$)$_3$OCH$_2$CH_2NH$_2$], 3.55–3.50 [m, 6 H, NCH$_2$CH$_2$(OCH_2CH$_2$)$_3$OCH$_2$CH$_2$NH$_2$], 3.46–3.40 [m, 6 H, NCH$_2$CH$_2$(OCH$_2$CH_2)$_3$OCH$_2$CH$_2$NH$_2$], 3.05–3.03 [t, *J* = 5.0 Hz, 2 H, NCH$_2$CH$_2$(OCH$_2$CH$_2$)$_3$OCH$_2$CH_2NH$_2$], 3.00–2.94 (dd, *J* = 17.5, 4.6 Hz, 1 H, H-4α), 2.85–2.80 (dd, *J* = 17.5, 1.8 Hz, 1 H, H-4β).

^{13}C NMR (125 MHz, CD_3OD): δ = 165.6, 156.50, 156.45, 155.8, 150.4, 145.3, 137.2, 132.3, 129.4, 125.6, 125.0, 108.9, 105.3, 97.8, 95.1, 94.5, 77.0, 70.05, 69.94, 69.88, 69.82, 69.78, 69.5, 69.0, 68.9, 66.3, 64.0, 50.1, 39.2, 25.5.

HRMS (ESI): *m*/*z* calcd for $C_{35}H_{42}N_4O_{15}Na$ [M + Na]$^+$: 781.2544; found: 781.2525.

(2*R*,3*R*)-5,7-Dihydroxy-2-(3,4,5-trihydroxyphenyl)chroman-3-yl 4-{[1-(17-Amino-3,6,9,12,15-pentaoxaheptadecyl)-1*H*-1,2,3-triazol-4-yl]methoxy}-3,5-dihydroxybenzoate (5e)

Compound was prepared according to GP2; yield: 29 mg (45%); white solid; mp, decomposed at >120 °C; $[\alpha]_D^{21}$ –79 (*c* = 0.1, MeOH).

FT-IR (neat): 3307, 2908, 1678, 1625, 1521, 1449, 1374, 1349, 1238, 1201, 1147, 1096, 845, 772, 722, 652, 633 cm^{-1}.

^{1}H NMR (500 MHz, CD_3OD): δ = 7.90 (s, 1 H, triazole-H), 6.87 (s, 2 H, Gal H-2, H-6), 6.49 (s, 2 H, H-2′, H-6′), 5.93 (s, 2 H, H-6. H-8), 5.52–5.53 (m, 1 H, H-3), 5.24 (s, 2 H, OCH_2R), 4.95 (s, 1 H, H-2), 4.52–4.50 [t, *J* = 4.7 Hz, 2 H, N$CH_2CH_2(OCH_2CH_2)_4OCH_2CH_2NH_2$], 3.82–3.71 [m, 2 H, $NCH_2CH_2(OCH_2CH_2)_4OCH_2CH_2NH_2$], 3.63–3.60 [m, 2 H, $NCH_2CH_2(OCH_2CH_2)_4OCH_2CH_2NH_2$], 3.57–3.38 [m, 16 H, $NCH_2CH_2(OCH_2CH_2)_4OCH_2CH_2NH_2$], 3.01–2.94 [m, 3 H, $NCH_2CH_2(OCH_2CH_2)_4OCH_2CH_2NH_2$, H-4α], 2.85–2.80 (dd, *J* = 17.5, 1.8 Hz, 1 H, H-4β).

^{13}C NMR (125 MHz, CD_3OD): δ = 165.6, 156.56, 156.49, 155.8, 150.4, 145.3, 143.6, 137.2, 132.3, 129.4, 125.6, 124.9, 108.9, 105.3, 97.8, 95.1, 94.5, 77.0, 69.94, 69.87, 69.84, 69.80, 69.76, 69.70, 69.68, 69.43, 69.0, 68.9, 66.3, 63.9, 50.0, 39.2, 25.5.

HRMS (ESI): *m*/*z* calcd for $C_{37}H_{47}N_4O_{16}$ [M + H]$^+$: 803.2987; found: 803.2997.

Conflict of Interest

The authors declare no conflict of interest.

Funding Information

Funding provided by the Donald J. and Jane M. Cram Endowment (to P.H.), the NIH (R56 AG070895 to D.E.), and the HHMI (D.E.).

Supporting Information

Supporting information for this article is available online at https://doi.org/10.1055/a-1509-5904.

References

(1) Present address: Department of Pharmacology and Pharmaceutical Sciences, University of Southern California School of Pharmacy, 1985 Zonal Ave, Los Angeles CA 90089-9121, USA.
(2) *Alzheimers Dement.* **2020**, *16*, 391.
(3) Gouras, G. K.; Olsson, T. T.; Hansson, O. *Neurotherapeutics* **2015**, *12*, 3.
(4) Murray, M. E.; Lowe, V. J.; Graff-Radford, N. R.; Liesinger, A. M.; Cannon, A.; Przybelski, S. A.; Rawal, B.; Parisi, J. E.; Petersen, R. C.; Kantarci, K.; Ross, O. A.; Duara, R.; Knopman, D. S.; Jack, C. R.; Dickson, D. W. *Brain* **2015**, *138*, 1370.
(5) (a) Bieschke, J.; Russ, J.; Friedrich, R. P.; Ehrnhoefer, D. E.; Wobst, H.; Neugebauer, K.; Wanker, E. E. *Proc. Natl. Acad. Sci. U. S. A.* **2010**, *107*, 7710. (b) Debnath, K.; Shekhar, S.; Kumar, V.; Jana, N. R.; Jana, N. R. *ACS Appl. Mater. Interfaces* **2016**, *8*, 20309.
(6) Wobst, H. J.; Sharma, A.; Diamond, M. I.; Wanker, E. E.; Bieschke, J. *FEBS Lett.* **2015**, *589*, 77.
(7) (a) Seidler, P. M.; Boyer, D. R.; Sawaya, M. R.; Ge, P.; Shin, W. S.; DeTure, M. A.; Dickson, D. W.; Jiang, L.; Eisenberg, D. S. *bioRxiv* **2020**, preprint DOI: 10.1101/2020.05.29.124537. (b) Sonawane, S. K.; Chidambaram, H.; Boral, D.; Gorantla, N. V.; Balmik, A. A.; Dangi, A.; Ramasamy, S.; Marelli, U. K.; Chinnathambi, S. *Sci. Rep.* **2020**, *10*, 12579.
(8) (a) Lu, M.; Cohen, M. H.; Rieves, D.; Pazdur, R. *Am. J. Hematol.* **2010**, *85*, 315. (b) Muldoon, L. L.; Sàndor, M.; Pinkston, K. E.; Neuwelt, E. A. *Neurosurgery* **2005**, *57*, 785. (c) Neubert, J.; Wagner, S.; Kiwit, J.; Bräuer, A. U.; Glumm, J. *Int. J. Nanomed.* **2015**, *10*, 2033. (d) Nguyen, K. L.; Yoshida, T.; Kathuria-Prakash, N.; Zaki, I. H.; Varallyay, C. G.; Semple, S. I.; Saouaf, R.; Rigsby, C. K.; Stoumpos, S.; Whitehead, K. K.; Griffin, L. M.; Saloner, D.; Hope, M. D.; Prince, M. R.; Fogel, M. A.; Schiebler, M. L.; Roditi, G. H.; Radjenovic, A.; Newby, D. E.; Neuwelt, E. A.; Bashir, M. R.; Hu, P.; Paul Finn, J. *Radiology* **2019**, *293*, 554.
(9) Wang, J.; Sun, P.; Wang, Q.; Zhang, P.; Wang, Y.; Zi, C.; Wang, X.; Sheng, J. *Cancer Cell Int.* **2019**, *19*, 266.
(10) Yang, Q.; Sheng, M.; Henkelis, J. J.; Tu, S.; Wiensch, E.; Zhang, H.; Zhang, Y.; Tucker, C.; Ejeh, D. E. *Org. Process Res. Dev.* **2019**, *23*, 2210.
(11) (a) Aufort, M.; Herscovici, J.; Bouhours, P.; Moreau, N.; Girard, C. *Bioorg. Med. Chem. Lett.* **2008**, *18*, 1195. (b) Dieterich, D. C.; Lee, J. J.; Link, A. J.; Graumann, J.; Tirrell, D. A.; Schuman, E. M. *Nat. Protoc.* **2007**, *2*, 532. (c) Floros, M. C.; Leão, A. L.; Narine, S. S. *BioMed Res. Int.* **2014**, Article ID 792901. (d) Lee, W.; Sarkar, S.; Pal, R.; Kim, J. Y.; Park, H.; Huynh, P. T.; Bhise, A.; Bobba, K. N.; Kim, K. I.; Ha, Y. S.; Soni, N.; Kim, W.; Lee, K.; Jung, J. M.; Rajkumar, S.; Lee, K. C.; Yoo, J. *ACS Appl. Biomater.* **2021**, *4*, 2544. (e) Sun, P.; Chen, J.; Liu, J.; Zhang, K. *Macromolecules* **2017**, *50*, 1463.
(12) Himo, F.; Lovell, T.; Hilgraf, R.; Rostovtsev, V. V.; Noodleman, L.; Sharpless, K. B.; Fokin, V. V. *J. Am. Chem. Soc.* **2005**, *127*, 210.
(13) Rostovtsev, V. V.; Green, L. G.; Fokin, V. V.; Sharpless, K. B. *Angew. Chem. Int. Ed.* **2002**, *41*, 2596.
(14) Chan, T. R.; Hilgraf, R.; Sharpless, K. B.; Fokin, V. V. *Org. Lett.* **2004**, *6*, 2853.
(15) Madhusudanan, K. P.; Sachdev, K.; Harrison, D. A.; Kulshreshtha, D. K. *Int. J. Mass Spectrom. Ion Processes* **1984**, *62*, 289.
(16) Jordheim, M.; Fossen, T.; Songstad, J.; Andersen, Ø. M. *J. Agric. Food Chem.* **2007**, *55*, 8261.
(17) (a) Sanders, D. W.; Kaufmann, S. K.; DeVos, S. L.; Sharma, A. M.; Mirbaha, H.; Li, A.; Barker, S. J.; Foley, A. C.; Thorpe, J. R.; Serpell, L. C.; Miller, T. M.; Grinberg, L. T.; Tolnay, M.; Seeley, W. W.; Diamond, M. I. *Neuron* **2014**, *82*, 1271. (b) Seidler, P. M.; Boyer, D. R.; Murray, K. A.; Yang, T. P.; Bentzel, M.; Sawaya, M. R.; Rosenberg, G.; Cascio, D.; Williams, C. K.; Newell, K. L.; Ghetti, B.; DeTure, M. A.; Dickson, D. W.; Vinters, H. V.; Eisenberg, D. S. *J. Biol. Chem.* **2019**, *294*, 16451.
(18) (a) Toth, G. B.; Varallyay, C. G.; Horvath, A.; Bashir, M. R.; Choyke, P. L.; Daldrup-Link, H. E.; Dosa, E.; Finn, J. P.; Gahramanov, S.; Harisinghani, M.; Macdougall, I.; Neuwelt, A.; Vasanawala, S. S.; Ambady, P.; Barajas, R.; Cetas, J. S.; Ciporen, J.; DeLoughery, T. J.; Doolittle, N. D.; Fu, R.; Grinstead, J.; Guimaraes, A. R.; Hamilton, B. E.; Li, X.; McConnell, H. L.; Muldoon, L. L.; Nesbit, G.; Netto, J. P.; Petterson, D.; Rooney, W. D.; Schwartz, D.; Szidonya, L.; Neuwelt, E. A. *Kidney Int.* **2017**, *92*, 47. (b) Enteshari Najafabadi, R.; Kazemipour, N.; Esmaeili, A.; Beheshti, S.; Nazifi, S. *BMC Pharmacol. Toxicol.* **2018**, *19*, 59.
(19) (a) He, A.; Guan, X.; Song, H.; Li, S.; Huang, K. *Food Biosci.* **2020**, *37*, 100727. (b) Radhakrishnan, R.; Kulhari, H.; Pooja, D.; Gudem, S.; Bhargava, S.; Shukla, R.; Sistla, R. *Chem. Phys. Lipids* **2016**, *198*, 51. (c) Sanna, V.; Singh, C. K.; Jashari, R.; Adhami, V.

M.; Chamcheu, J. C.; Rady, I.; Sechi, M.; Mukhtar, H.; Siddiqui, I. A. *Sci. Rep.* **2017**, *7*, 41573. (d) Smith, A.; Giunta, B.; Bickford, P. C.; Fountain, M.; Tan, J.; Shytle, R. D. *Int. J. Pharm.* **2010**, *389*, 207. (e) Zou, L-Q.; Peng, S-F.; Liu, W.; Gan, L.; Liu, W-L.; Liang, R-H.; Liu, C-M.; Niu, J.; Cao, Y-L.; Liu, Z.; Chen, X. *Food Res. Int.* **2014**, *64*, 492.

(20) Tran, F.; Odell, A. V.; Ward, G. E.; Westwood, N. J. *Molecules* **2013**, *18*, 11639.

(21) Friscourt, F.; Fahrni, C. J.; Boons, G. J. *J. Am. Chem. Soc.* **2012**, *134*, 18809.

(22) Bertozzi, C. R.; Bednarski, M. D. *J. Org. Chem.* **1991**, *56*, 4326.

(23) Brauch, S.; Henze, M.; Osswald, B.; Naumann, K.; Wessjohann, L. A.; Van Berkel, S. S.; Westermann, B. *Org. Biomol. Chem.* **2012**, *10*, 958.

(24) Wang, H.; Raghupathi, K. R.; Zhuang, J.; Thayumanavan, S. *ACS Macro Lett.* **2015**, *4*, 422.